

1   **Systems approaches provide new insights into**  
2   ***Arabidopsis thaliana* root growth under mineral nutrient**  
3   **limitation**

4  
5   Authors

6   **Nadia Bouain<sup>1</sup>, Arthur Korte<sup>2</sup>, Santosh B. Satbhai<sup>3,4†</sup>, Seung Y. Rhee<sup>5</sup>, Wolfgang**  
7   **Busch<sup>3,4</sup>, Hatem Rouached<sup>1,\*</sup>**

8  
9   **Affiliations**

10  
11   1-BPMP, Univ Montpellier, CNRS, INRA, SupAgro, Montpellier, France

12  
13   2-Evolutionary Genomics, Center for Computational and Theoretical Biology (CCTB),  
14   University Würzburg, Würzburg, Germany

15  
16   3-Gregor Mendel Institute (GMI), Austrian Academy of Sciences, Vienna Biocenter  
17   (VBC), Vienna, Austria

18  
19   4- Plant Molecular and Cellular Biology Laboratory, and Integrative Biology  
20   Laboratory, Salk Institute for Biological Studies, La Jolla, California, USA

21  
22   5- Department of Plant Biology, Carnegie Institution for Science, Stanford, California  
23   94305, USA

24  
25   Present address

26   †- Department of Biological Sciences, Indian Institute of Science Education and  
27   Research (IISER) Mohali, Punjab, India

28  
29   \* **Correspondence:** Hatem Rouached (hatem.rouached@inra.fr)

30    **Abstract (200)**

31  
32    The molecular genetic mechanisms by which plants modulate their root growth rate  
33    (RGR) in response to nutrient deficiency are largely unknown. Using a panel of  
34    *Arabidopsis thaliana* natural accessions, we provide a comprehensive combinatorial  
35    analysis of RGR variation under macro- and micronutrient deficiency, namely  
36    phosphorus (P), iron (Fe), and zinc (Zn), which affect root growth in opposite  
37    directions. We found that while -P stimulates early RGR of most accessions, -Fe or -  
38    Zn reduces it. The combination of either -P-Fe or -P-Zn leads to suppression of the  
39    growth inhibition exerted by -Fe or -Zn alone. Surprisingly, *Arabidopsis* reference  
40    accession Columbia (Col-0) is not representative of the species under -P and -Zn.  
41    Using a genome wide association study, we identify candidate genes that control  
42    RGR under the assayed nutrient deficiency conditions. By using a network biology  
43    driven search using these candidate genes, we further identify a functional module  
44    enriched in regulation of cell cycle, DNA replication and chromatin modification that  
45    possibly underlies the suppression of root growth reduction in -P-Fe conditions.  
46    Collectively, our findings provide a framework for understanding the regulation of  
47    RGR under nutrient deficiency, and open new routes for the identification of both  
48    large effect genes and favorable allelic variations to improve root growth.

49

50

51

52

53 **Introduction**

54  
55 Global climate change and population increase pose a tremendous challenge and  
56 prompt an urgent need for efficient agriculture and food production. The current  
57 projection is that the world population will be over 9.8 billion by 2050, and global food  
58 production will have to further increase by 70% to sustain this population (Tomlinson,  
59 2013). At the same time, climate change is associated with a decrease of important  
60 micronutrients such as iron (Fe) and zinc (Zn) in staple foods such as rice (Zhu et al.,  
61 2018). The bio-availability of Fe and Zn is often limited in the soil, leading to  
62 reductions in growth, crop yield, and quality. As plants are the entry point of these  
63 elements in the food web, low accumulation of these elements in plants is associated  
64 with malnutrition in humans. Zn and Fe deficiencies are estimated to affect up to 2  
65 billion people worldwide (Hilty et al., 2010). Moreover, modern industrialized  
66 agriculture has created a strong demand and dependency for fertilizers, posing the  
67 danger of acute limitation of non-renewable fertilizer components, in particular  
68 phosphorus (P) (Abelson 1999; Cordell et al., 2009; Neset and Cordell 2011). All  
69 these nutrients (P, Zn and Fe) are taken-up by plants at the root-soil interface, and  
70 plants often face conditions in which one or more of these elements are limiting  
71 (Shahzad et al., 2014; Bouain et al., 2016). Thus, improving the capacity of plants to  
72 absorb these nutrients from the soil is a major goal of crop improvement. The  
73 development of crops with higher tolerance for individual and multiple nutrient  
74 stresses is a direction towards more sustainable and efficient agriculture.

75  
76 P is an essential macronutrient for plant growth and development. P is a  
77 critical component of many macromolecules (e.g. DNA), energy sources (e.g. ATP)  
78 and regulation of signal transduction via phosphorylation (Poirier and Bucher, 2002;  
79 Rouached et al., 2010). Plants acquire P as soluble inorganic phosphate (Pi) by a  
80 suite of high affinity phosphate transporters in the root (Secco et al., 2017). In soil, P  
81 distribution is heterogeneous (Hanlon et al., 2018), and usually found in shallow soil  
82 layers (Heppell et al., 2016). To cope with P heterogeneity in soil, plants increase  
83 root growth in shallow soil layers that promote topsoil foraging, thereby conferring an  
84 advantage for P acquisition (Lynch, 2011; Miguel et al., 2013).

85  
86 The effects of P deficiency (-P) on the root system have been studied in many  
87 plant species. For the model plant *Arabidopsis thaliana* (*A. thaliana*), the accession

88 Columbia (Col-0) is commonly considered as the reference (Somssich et al., 2018).  
89 Changes that occur in root architecture in -P consist of reduction of primary root  
90 growth (PRG), an increase in the growth of secondary roots, and an increase in root  
91 hair length and density (for review, Bouain et al., 2016). A handful of genes involved  
92 in PRG under -P have been cloned. Under -P, mutants of these genes are  
93 characterized either by their ability to maintain PRG such as the *low phosphate root 1*  
94 (*lpr1*) mutants (Svistoonoff et al., 2007), or by a strong inhibitory effect of the PRG  
95 (hypersensitivity) such as the *phosphate deficiency response 2* (*pdr2*) mutants  
96 (Ticconi et al., 2004) and *hypersensitive to pi starvation 7* (*hps7*) (Kang et al., 2014).  
97 More genes involved in inhibition of PRG were recently identified, including a  
98 transcription factor SENSITIVE TO PROTON RHIZOTOXICITY (STOP1) and its  
99 target ALUMINUM ACTIVATED MALATE TRANSPORTER 1 (ALMT1) (Mora-Macías  
100 et al., 2017; Balzergue et al., 2017). In addition to genetic screens for mutants  
101 affected in their response to -P, *A. thaliana* has natural accessions that are either  
102 oversensitive (e.g. Shadara) or more tolerant (e.g. Landsberg *erecta*) to -P compared  
103 to Col-0 (Reymond et al., 2006). The existence of natural variation in root growth in  
104 response to -P indicates the potential for discovering new genes that control this trait  
105 via quantitative genetic approaches.  
106

107 Fe and Zn are involved in vital biological processes ensuring proper  
108 functioning of the cell. Fe is a cofactor for numerous enzymes and a part of Fe–S  
109 clusters that are a major sink for Fe and essential for many important cellular  
110 processes such as photosynthesis and respiration (White and Broadley, 2009;  
111 Couturier et al., 2013). Similarly, Zn functions as a cofactor for hundreds of enzymes  
112 (Sinclair and Krämer, 2012). Since Zn and Fe are taken up by roots, improvement of  
113 root growth could help increase Zn and Fe content in plants. In Col-0, deficiencies in  
114 Fe and Zn impose a change in root architecture in a contrasting manner (Gruber et  
115 al., 2013; Bouain et al., 2018). While Fe deficiency (-Fe) inhibits root elongation  
116 (Gruber et al., 2013; Satbhai et al. 2017), Zn deficiency (-Zn) slightly promotes early  
117 root growth (Bouain et al., 2018). Only few genes that regulate primary root growth  
118 under -Fe or -Zn conditions have been identified. For instance, mutations in the  
119 BASIC HELIX-LOOP-HELIX-TYPE transcription factors POPEYE (Long et al., 2010),  
120 or the two interacting transcription factors, bHLH34 and bHLH104 (Li et al., 2016),  
121 inhibited the primary root growth in -Fe. More genes that control root architecture

122 under -Fe and -Zn conditions remain to be identified. The convenience of genome-  
123 wide association studies (GWAS) in *A. thaliana* offers an opportunity to explore the  
124 diversity in the response of accessions to mineral nutrients and interactions between  
125 nutrients, which promises the identification of candidate genes and their genetic  
126 variants controlling these traits.

127

128       Recent research has shown that nutrient homeostasis by interaction between  
129 nutrients is a general rule in plants rather than an exception (for review, Briat et al.,  
130 2015; Rouached and Rhee, 2017). P and Zn or P and Fe interact in the plant, and  
131 these interactions are visible at the molecular level as revealed by transcriptome  
132 analyses, where the deficiency of one-element induces or represses genes involved  
133 in the regulation of the other element (Misson et al., 2004; Kellermeier et al., 2014;  
134 Bouain et al., 2014; Briat et al., 2015; Li and Lan, 2015). The response to -P or -Fe  
135 may share common hormone signals, such as cytokinin. For example, cytokinin  
136 signaling, mediated by the cytokinin receptors CYTOKININ RESPONSE 1/WOODEN  
137 LEG/ARABIDOPSIS HISTIDINE KINASE 4 (CRE1/WOL/AHK4), is involved in the  
138 response to -P or -Fe in *A. thaliana* (Col-0) (Martin et al., 2000; Franco-Zorrilla et al.,  
139 2005; Séguéla et al., 2008). The outcome of the interaction of these nutrients is also  
140 visible at the morphological level (Kellermeier et al., 2014). Perhaps the most  
141 prominent example is the -P-Fe interaction and its effect on root growth. Root growth  
142 inhibition in response to -P has been proposed to be the result of Fe “toxicity” (Ward  
143 et al., 2008; Bournier et al., 2013) and it has been suggested that the inhibition of  
144 Arabidopsis (Col-0) primary root growth under -P is due to a presumed  
145 overabundance of available Fe, and is not solely due to -P alone (Ward et al., 2008;  
146 Bournier et al., 2013). This Fe overabundance was proposed to depend on malate  
147 exudation and presumably malate chelating Fe. The malate transporter ALMT1 was  
148 shown to be involved in this process, likely by promoting Fe accumulation in the root  
149 meristem causing the inhibition of cell expansion under -P (Balzergue et al., 2017;  
150 Mora-Macias et al., 2017). Fe accumulation in the root tip of P-deficient plants was  
151 proposed to be the cause for the differentiation of the apical root meristem - possibly  
152 through a prevention of the symplastic cell-to-cell communication as a consequence  
153 of callose deposition (Mora-Macias et al., 2017). The PDR2-LPR1 module was  
154 proposed to mediate this callose accumulation in root meristems experiencing -P  
155 (Balzergue et al., 2017). It has been proposed that the CLAVATA3/ESR (CLE)-

156 related protein 14 precursor (CLE14) is the signal that triggers full root meristem  
157 differentiation in -P through CLV2/PEPR2 receptors (Gutiérrez-Alanís et al., 2017). It  
158 has been shown that the CLE14 pathway acts downstream of LPR1/LPR2  
159 (Gutiérrez-Alanís et al., 2017). In contrast, these cellular hallmarks of -P were not  
160 observed under simultaneous P and Fe deficiency. The callose deposition was not  
161 detected and root growth was comparable to plants grown under complete medium.  
162 Thus far, these two modules LPR1-PDR2 and STOP1-ALMT1 have been used to  
163 explain how P and Fe signals shape root growth under P and Fe deficient conditions  
164 (Balzergue et al., 2017; Mora-Macias et al., 2017; Abel et al., 2017; Gutierrez-Alanis  
165 et al., 2018).

166

167 Plants have evolved mechanisms to sense and respond to nutrient deficiency  
168 early in their life cycle. Soon after germination, roots are the main targets of nutrient  
169 deficiency stress. Root growth responses to nutrient changes are genetically  
170 determined, and vary between and within plant species (Ristova and Busch, 2014).  
171 Identifying genes and mechanisms that underlie natural variation of root growth has  
172 become possible through large-scale phenotyping and various mapping approaches  
173 (Slovak et al., 2016). Here we set out to investigate variation in the root growth rate  
174 (RGR) of a panel of natural accessions in *A. thaliana* under single and combined  
175 deficiencies of P, Fe, and Zn. We used GWAS to identify candidate genes involved in  
176 RGR regulation under each of the growth conditions tested. Finally, we used a  
177 network biology driven search using these candidate genes to identify potential  
178 networks and processes that are relevant for determining RGR under the nutrient  
179 deficiency conditions. Taken together, our findings shed light on the regulation of root  
180 growth by combinatorial mineral nutrient cues and provide a foundation for guiding  
181 new agronomical and biotechnological strategies to improve root growth.

182

### 183 **Results**

#### 184 **RGR responds distinctly to single and combined nutrient deficiencies in a 185 genotype dependent manner**

186

187 Natural variation of root system architecture was reported for -P (Chevalier et al.,  
188 2003; Reymond et al., 2006; Kawa et al., 2016) as well as for -Fe (Satbhai et al.,  
189 2016) and -Zn (Bouain et al., 2018), yet never for their combination (-P-Fe or -P-Zn).

190 In particular, root growth rate (RGR) as a trait has not been evaluated under any  
191 nutritional stresses. Therefore, we set out to explore the natural variation of RGR in  
192 *A. thaliana* by investigating the RGR of 227 genetically diverse natural accessions  
193 from the RegMap population (Horton et al., 2012) (Supplemental Table 1) grown on  
194 different media. We tested six growth conditions: control (Ct), deficiency of P (-P), Fe  
195 (-Fe), Zn (-Zn), P and Fe (-P-Fe), and P and Zn (-P-Zn) (Figure 1). Seedlings were  
196 imaged every day at the same time, and the primary root length (PRL) was  
197 determined using the BRAT software (Slovak et al., 2014). For each accession, we  
198 recorded the primary root length (PRL) of three, four and five-day old seedlings  
199 (Supplemental Table 1). We first examined the PRL of Columbia-0 (Col-0) accession  
200 under all growth conditions tested, as this accession is most widely used in  
201 Arabidopsis research. Consistent with previous studies (Gruber et al., 2013; Satbhai  
202 et al. 2017; Bouain et al., 2018), -P or -Fe caused a reduction of the Col-0 PRL,  
203 while -Zn slightly promoted it compared to the Ct condition (Figure 2). Also consistent  
204 with previously published results (Ward et al., 2008), the reduced PRL observed in -P  
205 was not observed in -P-Fe. A similar suppression of -P dependent growth rate  
206 reduction was observed in -P-Zn (Figure 2). Overall, the response of PRL in Col-0  
207 was consistent with previous reports, thus validating our experimental setup.

208 We next examined the whole set of accessions. To account for differences in  
209 germination of the accessions, we used RGR for all further comparisons. For this we  
210 conducted linear regression on the root length measurements, whereby the  
211 regression coefficient provided an estimate of the root growth rate in different  
212 treatments (Figure 1, Supplemental Table 1, 2). Under the assumption of linear  
213 growth during this early growth period, the regression coefficient on the replicates is  
214 an ideal measurement, and indeed the estimated slopes are significant for most  
215 accessions in most treatments (99.5% for -P, 98.7% for -PZn%, 97,8% for -PFe,  
216 96,5% for Ct, 93% for -Fe, 92,5% for -P-Zn) (Supplemental Table 1). Because the  
217 data sets were obtained simultaneously, they constitute a unique resource for  
218 comparing the RGRs between accessions. Our analysis revealed a large variation of  
219 RGR among the accessions in the control condition (Ct) and in response to each of  
220 the nutrient deficiency conditions (Figure 3). To test whether the variation of root  
221 growth is genetically determined, we analyzed the heritability ( $H^2$ ) (Lynch et al., 1998)  
222 of RGR using estimates from the mixed model. We found that the phenotypic  
223 variation for RGR in response to the different conditions is a highly heritable trait

224 (Supplemental Table 3). Like Col-0, the RGR of most accessions was reduced by -Fe  
225 treatment, and the extreme accessions included Zu-1, MIR-0, Rmx-A02, Edinburgh-  
226 5, and Ove-0. However, unlike Col-0, -Zn reduced RGR in most accessions, and the  
227 extreme accessions included Shadara, Sq-1, Sapporo-0, and Si-0. Here Col-0, which  
228 slightly increases RGR, was the exception to the rule. We found a similar surprise in -  
229 P. In -P, while Col-0 showed a reduction in their RGR, most accessions behaved in  
230 an opposite manner; their RGR was increased compared to Ct. When grown under  
231 combined nutrient deficiency (-P-Fe and -P-Zn), most accessions showed an RGR  
232 that was similar to the -P effect and distinct from -Fe or -Zn alone (Figure 3). P  
233 deficiency alleviated the RGR reduction mediated by Fe or Zn deficiency. Taken  
234 together, our analysis revealed that -P generally promoted early primary root growth  
235 whereas -Fe or -Zn reduced it in *A. thaliana*. In addition, removing P alleviated the  
236 root growth reduction brought on by Fe or Zn deficiency. This general response  
237 varied across natural accessions in response to single or combined nutrient  
238 deficiencies. Importantly, Col-0 was not the best representative accession for the  
239 responses in -P or -Zn conditions.

240  
241 **Distinct genetic architectures underlie the response to single and combined**  
242 **nutrient stresses in *Arabidopsis thaliana***

243 To determine the genomic loci that control RGR in response to mineral nutrient  
244 deficiencies, we performed GWAS using normalized RGRs (Figure 4, Supplemental  
245 Table 2). For each accession, normalized RGR was defined as the ratio between  
246 RGR from each nutrient deficiency condition divided by the RGR from the control  
247 condition (Ct). The significance of associations between phenotypes and the single  
248 nucleotide polymorphism (SNP) markers was evaluated using a linear mixed model  
249 (a modified version of EMMA) (Kang et al. 2008) that corrects for population  
250 structure. All considered normalized RGRs show low but a significant estimated  
251 heritability ( $H^2$ ) (Supplemental Table 3). We next used ~1.7 million markers with a  
252 minor allele frequency of at least 5% in the population and corrected the associated  
253 p-values for multiple hypothesis testing using a 5% Bonferroni threshold (Figure 4 A-  
254 E). Using this conservative threshold, and by taking into account genes present in a  
255 10kb window surrounding the underlying significant markers - acknowledging the  
256 rapid decay of LD in the *Arabidopsis* population (Gan et al., 2011) - we identified a  
257 list of 145 candidate genes (Supplemental Table 4) corresponding to 87 significant

258 SNPs in 32 distinct genomic regions (Supplemental Table 5). Of these, 96 genes (49  
259 SNPs) were associated with only one trait, while 31 genes (19 SNPs) were  
260 associated with two traits, and 18 genes (19 SNPs) were associated with 3 traits  
261 (Supplemental Table 4). Among these candidates, some are known to be involved in  
262 regulating root growth under mineral nutrient deficiency. For instance, the *CLV2* gene  
263 is known to trigger full root meristem differentiation under -P (Gutiérrez-Alanís et al.,  
264 2017) and was identified in our GWAS RGR on -P ( $p\text{-value}=2.1*10^{-8}$ ). Many  
265 candidate genes related to different classes of hormone signaling were also  
266 identified, including genes involved in auxin, gibberellin, cytokinin, ABA, and  
267 brassinosteroid pathways. For instance, the gene *BRASS/NAZOLE-RESISTANT 1*  
268 (*BZR1*,  $p=1.9*10^{-9}$ ) was identified to associate with the regulation of RGR under -Zn.  
269 Interestingly, there was a very limited overlap (if any) between the gene lists of single  
270 nutrient deficiencies (-P, -Zn, and -Fe) (Figure 4F). No common gene was detected  
271 between -P and -Fe, nor between -Fe and -Zn (Figure 4F, Supplemental Table 4).  
272 Only in the case of -P and -Zn, two overlapping regions (tagged by 17 SNPs)  
273 corresponding to 10 candidate genes were detected. The first region was significantly  
274 associated with -P-Zn, and the second region was associated with -P-Fe, in addition  
275 to -P and -Zn (Supplemental Table 6). The three associated SNPs in the first region,  
276 common between -P, -Zn, and -P-Zn, are in complete LD and tag the genes  
277 AT3G29570 and AT3G29575 ( $P\text{-values}$ : -P ( $p=2.1*10^{-8}$ ), -Zn ( $p=3.3*10^{-9}$ ), and -P-Zn  
278 ( $p=9.0*10^{-10}$ )). AT3G29575 is a member of the family of ABI five binding proteins  
279 (AFPs) and is involved in the stress response of germinating seeds and seedlings  
280 through modulation of ABA signaling (Garcia et al., 2008). Taken together, our  
281 GWAS analysis allowed the identification of interesting candidate genes that may  
282 underlie the natural variation of RGR in response to nutrient deficient conditions, and  
283 revealed that root growth responses to single stresses and to their combinations  
284 might be regulated by distinct genetic programs rather than being regulated in a  
285 simple additive manner.

286  
287 **The negative regulation of RGR by iron and zinc deficiencies is suppressed  
288 when combined with phosphate deficiency**

289 In line with the literature, we found that Col-0 plants grown under -P-Fe have longer  
290 primary roots compared to plants grown either on -P or -Fe (Figure 2). But, whether  
291 this compensation is a general mechanism of adaptation or just an exception for a

292 few accessions, and whether -P could also alleviate -Zn's negative effect on RGR in  
293 Arabidopsis remained unknown. We therefore set out to answer these questions. We  
294 compared normalized RGRs on combined nutrient stress (-P-Fe/Ct or -P-Zn/Ct) to  
295 normalized RGRs on single nutrient stress (-P/Ct, -Fe/Ct, or -Zn/Ct) (Figure 5 A-C).  
296 First, only a subset of accessions displayed a reduction of RGR on -P (e.g. Col-0,  
297 Sorbo, Rd-0, Rmx-A180, Mr-0, Hau-0, Got-22, Mdn-1, RRS-10) and they were  
298 compensated by the combined stress -P-Fe (Figure 5A, black dot for Col-0 and red  
299 dots for the rest). Second, reduction of RGR in -Fe was generally alleviated under  
300 combined stress of -P-Fe in *A. thaliana* accessions. Here the reference accession  
301 Col-0 behaved similarly to the majority of the accessions (Figure 5B, black dot).  
302 Finally, except for few accessions including Col-0, -P-Zn treatment generally caused  
303 a large compensation of RGR compared to -Zn (Figure 5C, black dot for Col-0). This  
304 compensation was widespread across accessions. A few examples of RGR  
305 compensation are shown for accessions such as Shadara, Sq-1, Sapporo-0, and Si-0  
306 (Figure 6). Taken together, our results indicate that the RGR inhibition of Fe and Zn  
307 deficiencies is alleviated by P deficiency as a general mechanism in this species.  
308

309 **Regulation of cell cycle and cell proliferation may be an important biological  
310 process underlying -P-Fe's compensation of -Fe mediated RGR reduction**

311 To gain insight on the genetic architecture of the mechanisms that mitigate -Fe or -  
312 Zn's inhibition of RGR by -P, we conducted GWAS to identify loci that were  
313 associated with the variation of RGR between double and single stresses. The traits  
314 we used are as follows:  $\Delta\text{RGR}_{(-\text{P-Fe}, -\text{Fe})} = \text{RGR}_{(-\text{P-Fe/Ct})} - \text{RGR}_{(-\text{Fe/Ct})}$ , and  $\Delta\text{RGR}_{(-\text{P-Zn}, -\text{Zn})} = \text{RGR}_{(-\text{P-Zn/Ct})} - \text{RGR}_{(-\text{Zn/Ct})}$  (Figure 7 A-B). While the heritability for  $\Delta\text{RGR}_{(-\text{P-Fe}, -\text{Fe})}$  was  
315 estimated as 0.27, the  $\Delta\text{RGR}_{(-\text{P-Zn}, -\text{Zn})}$  trait missed heritability. Consistently, using a  
316 conservative Bonferroni threshold, 4 regions spanning 21 candidate genes were  
317 identified for  $\Delta\text{RGR}_{(-\text{P-Fe}, -\text{Fe})}$  (Supplemental Table 6), and no candidate genes were  
318 associated for  $\Delta\text{RGR}_{(-\text{P-Zn}, -\text{Zn})}$ . From the 4 regions associated with  $\Delta\text{RGR}_{(-\text{P-Fe}, -\text{Fe})}$ , 3  
319 regions overlapped with QTLs identified in the previous analysis. The first region  
320 contains two genes, At2G05160 and AT2G05170, which were identified in the RGR  
321 for -P, -P-Fe and -P-Zn. The second and third regions span 7 and 8 genes, which  
322 were identified in the RGR for in -P-Fe and -P-Zn respectively. More importantly, the  
323 fourth region is specific to the  $\Delta\text{RGR}_{(-\text{P-Fe}, -\text{Fe})}$  trait, and contains 4 candidate genes  
324

325 including AT5G23980 that encodes a FERRIC REDUCTION OXIDASE 4, known to  
326 be involved in Fe reduction and absorption (Bernal et al., 2012).

327 We further analyzed the genetic architectures of both traits,  $\Delta\text{RGR}_{(-\text{P-Fe}, -\text{Fe})}$  and  
328  $\Delta\text{RGR}_{(-\text{P-Zn}, -\text{Zn})}$ , by using a less stringent P value threshold. We chose  $-\log_{10}(P) < 4$   
329 threshold as it is frequently used in similar studies (e.g. Davila Olivas et al., 2016;  
330 Thoen et al., 2017). Our analysis found 949 and 437 associated markers (SNP)  
331 corresponding to 186 genes and 92 genes for  $\Delta\text{RGR}_{(-\text{P-Fe}, -\text{Fe})}$  and  $\Delta\text{RGR}_{(-\text{P-Zn}, -\text{Zn})}$   
332 respectively (Supplemental Table 7). Among the genes detected for  $\Delta\text{RGR}_{(-\text{P-Fe}, -\text{Fe})}$ ,  
333 we found *VITAMINC4* (*VTC4*), a gene encoding a protein with dual myo-inositol-  
334 monophosphatase and ascorbate synthase activity involved in the reduction of  $\text{Fe}^{+3}$   
335 to produce the  $\text{Fe}^{+2}$  (Torabinejad et al., 2009). Interestingly, *VTC4* belongs to the set  
336 of genes that are direct targets of the PHOSPHARE RESPONSE1 (PHR1) (Bustos et  
337 al., 2010), and is considered as a potential candidate for the cross-talk between Fe  
338 and P signaling to regulate root growth (Mora-Macías et al., 2017). An overlap of 31  
339 SNPs (Supplemental Table 8) that correspond to 10 genes was detected  
340 (Supplemental Table 9) was detected for  $\Delta\text{RGR}_{(-\text{P-Fe}, -\text{Fe})}$  and  $\Delta\text{RGR}_{(-\text{P-Zn}, -\text{Zn})}$ . This  
341 overlap is significantly higher compared to random markers ( $p=2.8^{-11}$ ) or  
342 permutations for which no significant overlap at this threshold was observed. In this  
343 list we can distinguish in particular many genes involved in the transcriptional  
344 regulation (e.g. AT1G27730, *SALT TOLERANCE ZINC FINGER*; AT1G27660,  
345 *bHLH110*) and key gene involved in the DNA methylation (AT1G57820, *VARIANT IN*  
346 *METHYLATION 1*).

347 To capitalize upon our GWAS results, and to go beyond our *a priori* gene list  
348 to find pathways and functional modules that explain the variation of RGR, we took  
349 advantage of the existence of genome-scale gene co-function networks such as  
350 AraNetv2 that covers 84% of *A. thaliana*'s coding genes (Lee et al., 2015). Using this  
351 tool and all GWAS candidate genes for the  $\Delta\text{RGR}_{(-\text{P-Fe}, -\text{Fe})}$  trait, we identified three  
352 modules (Supplemental Table 10). The largest module comprises 26 genes  
353 connected with one another (Figure 8). The Gene Ontology (GO) annotation analysis  
354 revealed that there is significant enrichment for "chromatin modification" ( $p=2.44*10^{-6}$ ),  
355 "DNA replication" ( $p=9.58*10^{-5}$ ), and "regulation of cell cycle" ( $3.37*10^{-4}$ ) within  
356 this module. A similar analysis for genes associated with  $\Delta\text{RGR}_{(-\text{P-Zn}, -\text{Zn})}$  showed one  
357 module comprising 6 genes (Supplemental Table 12) with a significant GO  
358 enrichment for the "regulation of cell cycle" ( $p=2.8*10^{-6}$ ) and "cell proliferation"

359 (p=3.85\*10-6) (Supplemental Table 10). Taken together, our analyses suggest that  
360 similar molecular mechanisms may be involved in promoting RGR under different  
361 combined nutrient deficiency.

362  
363 **Discussion**

364 Below ground, roots can sense and respond to the nutrient stress during all phases  
365 of plant growth and development (Schachtman and Shin, 2007). An important part of  
366 this response is adjustment of the root growth rate in response to nutrient availability  
367 (López-Bucio et al., 2003; Osmont et al., 2007; Kellermeier et al., 2014). This  
368 plasticity of root growth is an important adaptive trait. Nevertheless, despite its  
369 primary importance for optimizing root foraging for resources in heterogeneous soil  
370 environments and ensuring crop yield, most of the work on plant mineral nutrition has  
371 focused on responses to absence of single nutrients, and the few studies that went  
372 beyond this did examined these responses only in a single strain (e.g. Kellermeier et  
373 al., 2014). Here, we report the first extensive analysis of the RGR in 227 accessions  
374 of *A. thaliana* grown under six nutritional conditions including combinatorial nutrient  
375 deficiencies: control (MS, Ct), -P, -Fe, -Zn, -P-Fe, and -P-Zn. We focused on the  
376 variation of RGR in an early phase of plant development given its fundamental  
377 importance in the plant life cycle. We showed the presence of a large amount of  
378 heritable natural variation of RGR under each growth condition. We then performed 7  
379 GWAS to look for the genetic variants underlying the observed natural variation of  
380 RGR, and present all significant associations. These data provide an insight into the  
381 genetic basis that underlies root growth responses to multiple nutrient deficiencies  
382 and lay a firm foundation to identify and characterize causative polymorphisms  
383 through functional molecular work.

384  
385 Genetic differences between *A. thaliana* accessions underlie the plant's  
386 extensive phenotypic variation, and until now these have been interpreted largely in  
387 the context of the Col-0 accession. While Col-0 has been the predominant natural  
388 accession for research in plant biology for many decades (Somssich et al., 2018).  
389 Our work provides clear evidence that Col-0 is not the best representative of the  
390 species for P and Zn deficiency responses, which is highly relevant because Col-0  
391 responses were often assumed to be the general responses of plants to nutrient  
392 deficiencies. Unlike Col-0, most of the accessions reduce the RGR under -Zn, and  
393 more importantly most of the accessions stimulate the RGR under -P. This result

394 indicates that Col-0 is not the ideal accession to study all types of nutrient stresses.  
395 In -P, while Col-0 consistently showed a reduction of primary root growth in many  
396 studies, the amplitude of such RGR reduction varied largely between studies. For  
397 example, in Reymond et al., (2006) Col-0 exhibited a strong response to -P (5 µM P),  
398 whereas in Chevalier et al. (2003) (1 µM P), the primary root is only slightly affected.  
399 Reversely, the Shadara accession showed invariably an oversensitivity to -P  
400 conditions (Reymond et al., 2006; Svistoonoff et al., 2007; Shahzad et al., 2018),  
401 which was also observed in our study. This response in Shadara was used to  
402 generate a RIL population (using Bay-0 displaying long root under -P compared to  
403 Shadara as the other parent) that allowed the mapping of a key gene regulating root  
404 growth under -P, *LPR1* (Reymond et al., 2006). Despite its contrasting and consistent  
405 root growth responses to -P compared to Col-0, Shadara remains little used to study  
406 responses to -P. In our study, we examined the RGR in the early stages of plant  
407 development in response to -P, and thereby revealed that many accessions sense  
408 and respond to depletion of P in the medium by stimulating RGR. As these responses  
409 were observed early on during plant development, when P levels in the seedlings will  
410 not be significantly depleted, our result suggests the existence of mechanisms that  
411 perceive changes in P and contribute to early RGR modulation by -P. These  
412 mechanisms remain to be discovered, but once discovered, might be exploited to  
413 design strategies to improve root growth under -P.  
414

415 Most accessions displayed a reduction in the RGR under -Fe or -Zn  
416 conditions. However, the extent of this reduction varied between -Fe and -Zn with –  
417 Fe causing more reduction in general. Interestingly, when each of those single  
418 deficiency conditions was combined with -P, we observed an increase of RGR for  
419 most of the accessions. This indicates the existence of strong interdependencies of  
420 the root growth responses between the macronutrient P and micronutrients Fe and  
421 Zn. In line with our result, Rai et al., (2015) showed that the primary root length was  
422 significantly increased in response to -Fe-P compared to -Fe in Col-0. Furthermore, it  
423 has been well documented that -Fe or -Zn leads to the accumulation of P in plants  
424 (Rai et al., 2015; Khan et al., 2017; Kisko et al., 2018) likely through the activation of  
425 root Pi uptake (Huang et al., 2000, Kisko et al., 2018). Whether the accumulation of P  
426 in -Zn or -Fe conditions is directly related to the reduction of RGR will need further  
427 investigations. Conversely, plant over-accumulates Fe in -P conditions. As

428 aforementioned, it has been proposed that the Fe over-accumulation in Col-0 roots  
429 could reach a “toxic” level that cause the inhibition of root growth in -P. Consistently,  
430 the primary root growth grown under simultaneous absence of Fe and P is  
431 comparable to those observed under control condition (Ward et al., 2008; Balzergue  
432 et al., 2017; Mora-Macias et al., 2017; Abel et al., 2017; Gutierrez-Alanis et al.,  
433 2018). Our results confirm the observation made for Col-0, and extend it to other  
434 accessions (e.g. Shadara, Sorbo, Rd-0, Rmx-A180, Mr-0, Hau-0, Got-22, Mdn-1,  
435 RRS-10). Nevertheless, interestingly, this rescue of RGR by the additional absence  
436 of -Fe was not observed in most of the accession that we tested. Many accessions  
437 exhibited a reduction of RGR by -P-Fe compared to -P alone. This result suggests  
438 that the availability of Fe in the medium is not the sole determinant that control RGR  
439 under -P condition. Identification of mechanism(s) that control root growth under  
440 simultaneous -P-Fe deficiency deserves further research.

441 Taken together, our results show that there are multiple, genetically  
442 determined strategies for how plants respond to nutrient limitations. It is therefore  
443 difficult to generalize observations made on one single accession such as Col-0 to  
444 the species level. A more comprehensive strategy to study a variety of accessions is  
445 currently becoming feasible thanks to the availability of the genome sequence of  
446 thousands of accessions, and the possibility to generate mutations in genes of  
447 interest via gene editing technologies. Our results further highlight the importance of  
448 studying combined nutrient stresses to comprehensively understand plant responses  
449 to nutrient deficiency stresses and their underlying genetic and molecular  
450 mechanisms.

451  
452 Our data revealed an important aspect of plant responses to combined  
453 stresses. The overlap between GWAS candidate genes from two single stresses and  
454 their combination is very limited. This result strongly suggests that there is a distinct  
455 genetic architecture underlying the responses to single and combined nutrient  
456 stresses in plants. This is further supported by recent work exploring natural variation  
457 in *Arabidopsis* in response to abiotic (drought) or biotic (fungal pathogen) stresses,  
458 which indicated that distinct genetic mechanisms underlie responses to single and  
459 combined stresses (Davila Olivas et al., 2016). This finding is relevant for designing  
460 strategies to improve crop yields in the field, as natural environments impose multiple  
461 stresses at once. In particular, for gene stacking approaches deploying multiple

462 genes or alleles to help crops growing in the field that face multiple stresses, our data  
463 are in favor of using multiple “specialized genes” for combined stresses rather than  
464 stacking genes addressing individual stresses (Halpin, 2005). The “specialized  
465 genes” could be revealed through quantitative genetics approaches such as GWAS.  
466

467 Time and cost-efficiency of GWAS has made it a useful approach to  
468 understand the genetic and molecular factors that govern complex traits, such as the  
469 root growth under different nutritional conditions (Satbhai et al., 2017; Bouain et al.,  
470 2018). Our GWASs led to obtain lists of the most significant SNPs associated with  
471 the variation of RGR under each of the aforementioned six nutrient-deficient  
472 conditions. We then identified candidate genes covered by the GWAS QTLs. Some  
473 genes that are known to be involved in the regulation of Col-0 root growth under  
474 specific nutrient stress conditions were detected with modest p-values. For example,  
475 key genes known to regulate root growth under -P or -Fe have been detected,  
476 namely *HPS7* ( $p=3.83*10^{-6}$ ) (Kang et al., 2014) for -P, and *bHLH104* ( $p=2.3*10^{-6}$ ) for -  
477 Fe (Li et al., 2016). Interestingly, the well-characterized *LPR1* gene was identified  
478 among the GWAS candidate genes on RGR under -P ( $p= 8.18*10^{-5}$ ), -P-Fe ( $p=$   
479  $2.57*10^{-5}$ ), and on  $\Delta$ RGR (P-Fe, -Fe) ( $p= 3. 2*10^{-5}$ ). The *lpr1* mutant under -P is  
480 characterized by not only its longer primary root, but also its lower Fe content  
481 compared to wild-type plants (Balzergue et al., 2017). Nevertheless, whether the  
482 lower Fe content in *lpr1* is enough to trigger Fe deficiency signaling is unknown. If  
483 this hypothesis were confirmed, LPR1 would play an important role in integrating  
484 both Fe and P signals to control the primary root elongation. This hypothesis is  
485 supported by the recovery of root growth in Col-0 under combined -P and -Fe  
486 stresses compared to -P alone (Ward et al., 2008).

487 Beyond the root growth related genes, our GWAS identified many new  
488 candidate genes that were previously unknown to regulate RGR under single or  
489 combined nutrient deficiency. Nevertheless, it is important to go beyond the detection  
490 of candidate genes by GWAS either by functional validation of top ranked candidates  
491 based on p-values, or through to the identification of pathways and functional  
492 modules that explain complex traits. Starting with a list of candidate genes detected  
493 by GWAS for the compensation of RGR under -P-Fe/Ct compared to -Fe/Ct or under  
494 -P-Zn/Ct compared to -Zn/Ct described in this work, and by using a genome-scale  
495 gene co-function network AraNet (Lee et al., 2014), we predicted pathways that might

496 underlie the compensation strategy. Four statistically enriched biological processes  
497 included the regulation of cell cycle, chromatin modification, cell proliferation, and  
498 DNA replication. These biological processes can be subjected to perturbation to  
499 validate their role in the compensatory mechanism seen under -P-Fe or -P-Zn for  
500 RGR. Such systems genetics strategy will accelerate future research discovery  
501 leading to the improvement of our understanding of the regulation of root growth  
502 under single and combined nutrient deficiency.

503

## 504 **Materials and Methods**

505

### 506 *Plant materials and growth conditions*

507

508 A total of 227 natural accessions of *A. thaliana* (S Table 1) were phenotyped and  
509 used to perform GWAS. Six growth conditions were used, MS (Control; Ct),  
510 phosphate deficiency (-Pi), iron deficiency (-Fe), zinc deficiency (-Zn), phosphate and  
511 iron deficiency (-Pi-Fe) and phosphate and zinc deficiency (-Pi-Zn). Seeds were  
512 surface-sterilized in chlorine gas for 1 h. Chlorine gas was generated from 130 ml  
513 of 10% sodium hypochlorite and 3.5 ml of 37% hydrochloric acid. After sterilization,  
514 seeds were imbibed in water and stratified for 3 days at 4 °C in the dark to promote  
515 uniform germination. For each genotype we sowed 12 seeds, distributed on 4  
516 different plates. Each plate contained eight different accessions with 3 plants per  
517 accession. Plates were placed in the growth chamber in a randomized manner.  
518 Seeds were then germinated and grown vertically on 1X MS-agar medium, which  
519 contained 1 mM KH<sub>2</sub>PO<sub>4</sub>, 1 mM MgSO<sub>4</sub>, 0.5 mM KNO<sub>3</sub>, 0.25 mM Ca(NO<sub>3</sub>)<sub>2</sub>, 10 µM  
520 MnCl<sub>2</sub>, 30 µM H<sub>3</sub>BO<sub>3</sub>, 1 µM CuCl<sub>2</sub>, 0.1 µM (NH<sub>4</sub>)<sub>6</sub>Mo<sub>7</sub>O<sub>24</sub>, 50 µM KCl, 100 µM  
521 NaFeEDTA and 15 µM ZnSO<sub>4</sub> in presence of 0.8% (wt/vol) agar and 1 % (wt/vol)  
522 sucrose. -Pi medium was made by replacing the source of Pi (KH<sub>2</sub>PO<sub>4</sub>) to with 1 mM  
523 KH<sub>2</sub>CaCO<sub>3</sub>. -Zn medium was made by omitting the source of Zn (ZnSO<sub>4</sub>) in the  
524 medium. -P-Zn medium was made by not adding the only source of Zn (ZnSO<sub>4</sub>) and  
525 by replacing KH<sub>2</sub>PO<sub>4</sub> with 1 mM KH<sub>2</sub>CaCO<sub>3</sub> to the medium. -Fe medium was made  
526 by not adding the FeEDTA in the medium and by supplying the FerroZine that is  
527 known as a strong Fe chelator. -P-Fe medium was made by not adding the source of  
528 Fe (FeEDTA) and by supplying the FerroZine, and by replacing P source (KH<sub>2</sub>PO<sub>4</sub>)  
529 by 1mM KH<sub>2</sub>CaCO<sub>3</sub> to the medium. Plants were grown at 22°C in the same growth

530 chambers under the same light regime (long-day: 8 h dark, 16 h light) conditions.  
531 Plant phenotyping for GWAS was performed as described previously (Slovak et al.,  
532 2014). The BRAT software was used to perform root trait quantification (Slovak et al.,  
533 2014).

534

535 *Genome wide association studies (GWAS)*

536

537 Genome-wide association mapping was performed on the regression coefficients of  
538 root growth of three-, four- and five-days-old seedlings grown under the above  
539 detailed conditions. The phenotypic data for the rare root growth and the regression  
540 coefficients used in the analysis are available at the AraPheno database (Seren et  
541 al., 2016). The genotypic data were based on whole genome sequencing data [The  
542 1001 Genomes Consortium, 2016] and covered 4,932,457 SNPs for the 227  
543 accessions. 1,739,142 of these markers had a minor Allele frequency of at least 5%  
544 in the population and where further used for GWAS. GWAS was performed with a  
545 mixed model correcting for population structure in a two- step procedure, where first  
546 all markers where analyzed with a fast approximation (emmaX, [Kang et al. 2010])  
547 and afterwards the top 1000 markers where reanalyzed with the correct full model.  
548 The kinship structure has been calculated under the assumption of the infinitesimal  
549 model using all genetic markers with a minor Allele Frequency of more than 5 % in  
550 the whole population. The analysis was performed in R (R Core Team (2016)). The  
551 used R scripts are available at <https://github.com/arthurkorte/GWAS>. The Genotype  
552 Data used for GWAS are available [www.1001genomes.org](http://www.1001genomes.org).

553

554 Heritability estimates have been extracted from the mixed model according to the  
555 formula:  $H^2 = V_G / (V_G + V_E)$ , where  $V_G$  is the among-genotype variance component  
556 and  $V_E$  is the residual (error) variance.

557

558 *Molecular pathway prediction*

559

560 The functional modules were predicted based on the GWAS genes using the publicly  
561 available resource AraNet (Lee et al., 2015). Network visualization was generated  
562 using Cytoscape software (Shannon et al., 2003).

563

**References**

- 564 Abelson, P.H. (1999). A potential phosphate crisis. *Science* 283:2015-2015.
- 565 Alonso-Blanco, C., Andrade, J., Becker, C., Bemm, F., Bergelson, J., Borgwardt,  
566 K.M., Cao, J., Chae, E., Dezwaan, T.M., and Ding, W. (2016). 1,135 genomes  
567 reveal the global pattern of polymorphism in *Arabidopsis thaliana*. *Cell*  
568 166:481-491.
- 569 Balzergue, C., Darteville, T., Godon, C., Laugier, E., Meisrimler, C., Teulon, J.-M.,  
570 Creff, A., Bissler, M., Brouchoud, C., Hagège, A., et al. (2017). Low phosphate  
571 activates STOP1-ALMT1 to rapidly inhibit root cell elongation. *Nature Communications* 8:15300.
- 572 Bernal, M., Casero, D., Singh, V., Wilson, G. T., Grande, A., Yang, H., ... & Merchant,  
573 S. S. (2012). Transcriptome sequencing identifies SPL7-regulated copper  
574 acquisition genes FRO4/FRO5 and the copper dependence of iron  
575 homeostasis in *Arabidopsis*. *The Plant Cell* 24: 738-761.
- 576 Bouain, N., Satbhai, S.B., Korte, A., Saenchai, C., Desbrosses, G., Berthomieu, P.,  
577 Busch, W., and Rouached, H. (2018). Natural allelic variation of the AZI1 gene  
578 controls root growth under zinc-limiting condition. *PLoS Genet* 14:e1007304.
- 579 Bouain, N., Shahzad, Z., Rouached, A., Khan, G.A., Berthomieu, P., Abdelly, C.,  
580 Poirier, Y., and Rouached, H. (2014). Phosphate and zinc transport and  
581 signalling in plants: toward a better understanding of their homeostasis  
582 interaction. *Journal of experimental botany* 65:5725-5741.
- 583 Bournier, M., Tissot, N., Mari, S., Boucherez, J., Lacombe, E., Briat, J.-F., and  
584 Gaymard, F. (2013). *Arabidopsis ferritin 1 (AtFer1)* gene regulation by the  
585 phosphate starvation response 1 (AtPHR1) transcription factor reveals a direct  
586 molecular link between iron and phosphate homeostasis. *Journal of Biological  
587 Chemistry* 288:22670-22680.
- 588 Briat, J.-F., Rouached, H., Tissot, N., Gaymard, F., and Dubos, C. (2015). Integration  
589 of P, S, Fe, and Zn nutrition signals in *Arabidopsis thaliana*: potential  
590 involvement of PHOSPHATE STARVATION RESPONSE 1 (PHR1). *Frontiers  
591 in Plant Science* 6:290.
- 592 Bustos, R., Castrillo, G., Linhares, F., Puga, M. I., Rubio, V., Pérez-Pérez, J., ... &  
593 Paz-Ares, J. (2010). A central regulatory system largely controls transcriptional  
594 activation and repression responses to phosphate starvation in *Arabidopsis*.  
595 *PLoS Genetics*, 6(9), e1001102.
- 596 Chevalier, F., Pata, M., Nacry, P., Doumas, P., and Rossignol, M. (2003). Effects of  
597 phosphate availability on the root system architecture: large-scale analysis of  
598 the natural variation between *Arabidopsis* accessions. *Plant, Cell &  
599 Environment* 26:1839-1850.
- 600 Couturier, J., Touraine, B., Briat, J.-F., Gaymard, F., and Rouhier, N. (2013). The  
601 iron-sulfur cluster assembly machineries in plants: current knowledge and  
602 open questions. *Frontiers in Plant science* 4:259.
- 603 Davila Olivas, N.H., Kruijer, W., Gort, G., Wijnen, C.L., Loon, J.J., and Dicke, M.  
604 (2017). Genome-wide association analysis reveals distinct genetic  
605 architectures for single and combined stress responses in *Arabidopsis*  
606 *thaliana*. *New Phytologist* 213:838-851.
- 607 Franco-Zorrilla, J.M., Martín, A.C., Leyva, A., and Paz-Ares, J. (2005). Interaction  
608 between phosphate-starvation, sugar, and cytokinin signaling in *Arabidopsis*  
609 and the roles of cytokinin receptors CRE1/AHK4 and AHK3. *Plant physiology*  
610 138:847-857.
- 611
- 612
- 613

- 614 Gan, X., Stegle, O., Behr, J., Steffen, J. G., Drewe, P., Hildebrand, K. L., ... & Kahles,  
615 A. (2011). Multiple reference genomes and transcriptomes for *Arabidopsis*  
616 *thaliana*. *Nature*, 477:419-23.
- 617 Garcia, M.E., Lynch, T., Peeters, J., Snowden, C., and Finkelstein, R. (2008). A small  
618 plant-specific protein family of ABI five binding proteins (AFPs) regulates  
619 stress response in germinating *Arabidopsis* seeds and seedlings. *Plant*  
620 *molecular biology* 67:643-658.
- 621 Gruber, B.D., Giehl, R.F., Friedel, S., and von Wirén, N. (2013). Plasticity of the  
622 *Arabidopsis* root system under nutrient deficiencies. *Plant Physiology* 163:161-  
623 179.
- 624 Gutiérrez-Alanís, D., Yong-Villalobos, L., Jiménez-Sandoval, P., Alatorre-Cobos, F.,  
625 Oropeza-Aburto, A., Mora-Macías, J., Sánchez-Rodríguez, F., Cruz-Ramírez,  
626 A., and Herrera-Estrella, L. (2017). Phosphate starvation-dependent iron  
627 mobilization induces CLE14 expression to trigger root meristem  
628 differentiation through CLV2/PEPR2 signaling. *Developmental cell* 41:555-  
629 570.
- 630 Gutiérrez-Alanís, D., Ojeda-Rivera, J. O., Yong-Villalobos, L., Cárdenas-Torres, L., &  
631 Herrera-Estrella, L. (2018). Adaptation to Phosphate Scarcity: Tips from  
632 *Arabidopsis* Roots. *Trends in plant science* 23:721-730.
- 633 Halpin, C. (2005). Gene stacking in transgenic plants—the challenge for 21st century  
634 plant biotechnology. *Plant biotechnology journal* 3:141-155.
- 635 Hanlon, M.T., Ray, S., Saengwilai, P., Luthe, D., Lynch, J.P., and Brown, K.M.  
636 (2018). Buffered delivery of phosphate to *Arabidopsis* alters responses to low  
637 phosphate. *Journal of experimental botany* 69:1207-1219.
- 638 Heppell, J., Talboys, P., Payvandi, S., Zygalakis, K., Fliege, J., Withers, P., Jones, D.,  
639 and Roose, T. (2015). How changing root system architecture can help tackle  
640 a reduction in soil phosphate (P) levels for better plant P acquisition. *Plant, cell*  
641 & environment 38:118-128.
- 642 Heberle, H., Meirelles, G.V., da Silva, F.R., Telles, G.P., and Minghim, R. (2015).  
643 InteractiVenn: a web-based tool for the analysis of sets through Venn  
644 diagrams. *BMC bioinformatics* 16:169.
- 645 Hilty, F.M., Arnold, M., Hilbe, M., Teleki, A., Knijnenburg, J.T., Ehrensperger, F.,  
646 Hurrell, R.F., Pratsinis, S.E., Langhans, W., and Zimmermann, M.B. (2010).  
647 Iron from nanocompounds containing iron and zinc is highly bioavailable in rats  
648 without tissue accumulation. *Nature nanotechnology* 5:374-80.
- 649 Horton, M. W., Hancock, A. M., Huang, Y. S., Toomajian, C., Atwell, S., Auton, A., ...  
650 & Nordborg, M. (2012). Genome-wide patterns of genetic variation in  
651 worldwide *Arabidopsis thaliana* accessions from the RegMap panel. *Nature*  
652 *genetics*, 44:212-216.
- 653 Huang, C., Barker, S.J., Langridge, P., Smith, F.W., and Graham, R.D. (2000). Zinc  
654 deficiency up-regulates expression of high-affinity phosphate transporter  
655 genes in both phosphate-sufficient and-deficient barley roots. *Plant Physiology*  
656 124:415-422.
- 657 Kang, J., Yu, H., Tian, C., Zhou, W., Li, C., Jiao, Y., and Liu, D. (2014). Suppression  
658 of photosynthetic gene expression in roots is required for sustained root  
659 growth under phosphate deficiency. *Plant physiology* 165:1156-1170.
- 660 Kawa, D., Julkowska, M., Sommerfeld, H.M., ter Horst, A., Haring, M.A., and  
661 Testerink, C. (2016). Phosphate-dependent root system architecture  
662 responses to salt stress. *Plant physiology* 172:690-706.
- 663 Kellermeier, F., Armengaud, P., Seditas, T.J., Danku, J., Salt, D.E., and Amtmann, A.

- (2014). Analysis of the root system architecture of *Arabidopsis* provides a quantitative readout of crosstalk between nutritional signals. *Plant Cell* 26:1480-1496.

Khan, G.A., Bouraine, S., Wege, S., Li, Y., De Carbonnel, M., Berthomieu, P., Poirier, Y., and Rouached, H. (2014). Coordination between zinc and phosphate homeostasis involves the transcription factor PHR1, the phosphate exporter PHO1, and its homologue PHO1; H3 in *Arabidopsis*. *Journal of experimental botany* 65:871-884.

Kisko, M., Bouain, N., Safi, A., Medici, A., Akkers, R.C., Secco, D., Fouret, G., Krouk, G., Aarts, M.G., and Busch, W. (2018). LPCAT1 controls phosphate homeostasis in a zinc-dependent manner. *eLife* 7:e32077.

Korte, A., Vilhjálmsdóttir, B.J., Segura, V., Platt, A., Long, Q., and Nordborg, M. (2012). A mixed-model approach for genome-wide association studies of correlated traits in structured populations. *Nature genetics* 44:1066-1071.

Lee, T., Yang, S., Kim, E., Ko, Y., Hwang, S., Shin, J., Shim, J.E., Shim, H., Kim, H., Kim, C., et al. (2014). AraNet v2: an improved database of co-functional gene networks for the study of *Arabidopsis thaliana* and 27 other nonmodel plant species. *Nucleic acids research* 43:D996-D1002.

Li, X., Zhang, H.M., Ai, Q., Liang, G., and Yu, D. (2016). Two bHLH transcription factors, bHLH34 and bHLH104, regulate iron homeostasis in *Arabidopsis thaliana*. *Plant physiology* 170:2478-93.

Li, W., and Lan, P. (2015). Genome-wide analysis of overlapping genes regulated by iron deficiency and phosphate starvation reveals new interactions in *Arabidopsis* roots. *BMC research notes* 8:555.

Long, T. A., Tsukagoshi, H., Busch, W., Lahner, B., Salt, D. E., & Benfey, P. N. (2010). The bHLH transcription factor POPEYE regulates response to iron deficiency in *Arabidopsis* roots. *The Plant Cell* 22:2219-36.

López-Bucio, J., Cruz-Ramírez, A., and Herrera-Estrella, L. (2003). The role of nutrient availability in regulating root architecture. *Current Opinion in Plant Biology* 6:280-287.

Lynch, J.P. (2011). Root phenes for enhanced soil exploration and phosphorus acquisition: tools for future crops. *Plant physiology* 156:1041-1049.

Lynch, M., and Walsh, B. (1998). Genetics and analysis of quantitative traits: Sinauer Sunderland, MA. Maloof, J.N. (2003). QTL for plant growth and morphology. *Current opinion in plant biology* 6:85-90.

Martín, A.C., Del Pozo, J.C., Iglesias, J., Rubio, V., Solano, R., De La Peña, A., Leyva, A., and Paz-Ares, J. (2000). Influence of cytokinins on the expression of phosphate starvation responsive genes in *Arabidopsis*. *The Plant Journal* 24:559-567.

Miguel, M., Widrig, A., Vieira, R., Brown, K., and Lynch, J. (2013). Basal root whorl number: a modulator of phosphorus acquisition in common bean (*Phaseolus vulgaris*). *Annals of botany* 112:973-982.

Misson, J., Thibaud, M.-C., Bechtold, N., Raghothama, K., and Nussaume, L. (2004). Transcriptional regulation and functional properties of *Arabidopsis* Pht1; 4, a high affinity transporter contributing greatly to phosphate uptake in phosphate deprived plants. *Plant molecular biology* 55:727-741.

Mora-Macías, J., Ojeda-Rivera, J.O., Gutiérrez-Alanís, D., Yong-Villalobos, L., Oropeza-Aburto, A., Raya-González, J., Jiménez-Domínguez, G., Chávez-Calvillo, G., Rellán-Álvarez, R., and Herrera-Estrella, L. (2017). Malate-dependent Fe accumulation is a critical checkpoint in the root developmental

- 714 response to low phosphate. *Proceedings of the National Academy of Sciences*  
715 of the United States of America 114:E3563-E3572.
- 716 Neset, T.S., and Cordell, D. (2012). Global phosphorus scarcity: identifying synergies  
717 for a sustainable future. *J Sci Food Agric* 92:2-6.
- 718 Osmont, K.S., Sibout, R., and Hardtke, C.S. (2007). Hidden branches: developments  
719 in root system architecture. *Annual Review of Plant Biology* 58:93-113.
- 720 Poirier, Y., and Bucher, M. (2002). Phosphate transport and homeostasis in  
721 *Arabidopsis*. *The Arabidopsis Book*:e0024.
- 722 Rai, V., Sanagala, R., Sinilal, B., Yadav, S., Sarkar, A.K., Dantu, P.K., and Jain, A.  
723 (2015). Iron availability affects phosphate deficiency-mediated responses, and  
724 evidence of cross-talk with auxin and zinc in *Arabidopsis*. *Plant and Cell  
725 Physiology* 56:1107-1123.
- 726 Reymond, M., Svistoonoff, S., Loudet, O., Nussaume, L., and Desnos, T. (2006).  
727 Identification of QTL controlling root growth response to phosphate starvation  
728 in *Arabidopsis thaliana*. *Plant, cell & environment* 29:115-125.
- 729 Rouached, H., Arpat, A.B., and Poirier, Y. (2010). Regulation of phosphate starvation  
730 responses in plants: signaling players and cross-talks. *Molecular Plant* 3:288-  
731 299.
- 732 Rouached, H., and Rhee, S.Y. (2017). System-level understanding of plant mineral  
733 nutrition in the big data era. *Current Opinion in System Biology* 4:71-77.
- 734 Satbhai, S.B., Setzer, C., Freynschlag, F., Slovak, R., Kerdaffrec, E., and Busch, W.  
735 (2017). Natural allelic variation of FRO2 modulates *Arabidopsis* root growth  
736 under iron deficiency. *Nature communications* 8:15603.
- 737 Schachtman, D.P., and Shin, R. (2007). Nutrient sensing and signaling: NPKS.  
738 *Annual Review of Plant Biology* 58:47-69.
- 739 Shannon P., Markiel A., Ozier O., Baliga N. S., Wang J. T., Ramage D., et al. (2003).  
740 Cytoscape: a software environment for integrated models of biomolecular  
741 interaction networks. *Genome Res.* 13 2498–2504.
- 742 Secco, D., Bouain, N., Rouached, A., Prom-U-Thai, C., Hanin, M., Pandey, A.K., and  
743 Rouached, H. (2017). Phosphate, phytate and phytases in plants: From  
744 fundamental knowledge gained in *Arabidopsis* to potential biotechnological  
745 applications in wheat. *Critical reviews in biotechnology* 37:898-910.
- 746 Séguéla, M., Briat, J.F., Vert, G., and Curie, C. (2008). Cytokinins negatively regulate  
747 the root iron uptake machinery in *Arabidopsis* through a growth-dependent  
748 pathway. *The Plant Journal* 55:289-300.
- 749 Shahzad, Z., Kellermeier, F., Armstrong, E. M., Rogers, S., Lobet, G., Amtmann, A.,  
750 & Hills, A. (2018). EZ-Root-VIS: A Software Pipeline for the Rapid Analysis  
751 and Visual Reconstruction of Root System Architecture. *Plant physiology*,  
752 177(4), 1368-1381.
- 753 Seren, Ü., Grimm, D., Fitz, J., Weigel, D., Nordborg, M., Borgwardt, K., & Korte, A.  
754 (2016). AraPheno: a public database for *Arabidopsis thaliana* phenotypes.  
755 *Nucleic acids research*, gkw986.
- 756 Sinclair, S.A., and Krämer, U. (2012). The zinc homeostasis network of land plants.  
757 *Biochimica et biophysica acta* 1823:1553-1567.
- 758 Slovak, R., Göschl, C., Su, X., Shimotani, K., Shiina, T., and Busch, W. (2014). A  
759 scalable open-source pipeline for large-scale root phenotyping of *Arabidopsis*.  
760 *The Plant Cell* 26:2390-2403.
- 761 Somssich, M. (2018). A short history of *Arabidopsis thaliana* (L.) Heynh. *Columbia-0:*  
762 *PeerJ Preprints*.
- 763 Svistoonoff, S., Creff, A., Reymond, M., Sigoillot-Claude, C., Ricaud, L., Blanchet, A.,

- 764 Nussaume, L., and Desnos, T. (2007). Root tip contact with low-phosphate  
765 media reprograms plant root architecture. *Nature Genetics* 39:792-796.  
766 Ticconi, C.A., Delatorre, C.A., Lahner, B., Salt, D.E., and Abel, S. (2004). Arabidopsis  
767 pdr2 reveals a phosphate-sensitive checkpoint in root development. *Plant  
768 Journal* 37:801-814.  
769 Thoen, M.P., Davila Olivas, N.H., Kloth, K.J., Coolen, S., Huang, P.P., Aarts, M.G.,  
770 Bac-Molenaar, J.A., Bakker, J., Bouwmeester, H.J., and Broekgaarden, C.  
771 (2017). Genetic architecture of plant stress resistance: multi-trait  
772 genome-wide association mapping. *New Phytologist* 213:1346-1362.  
773 Tomlinson, I. (2013). Doubling food production to feed the 9 billion: a critical  
774 perspective on a key discourse of food security in the UK. *Journal of rural  
775 studies* 29:81-90.  
776 Torabinejad, J., Donahue, J.L., Gunesekera, B.N., Allen-Daniels, M.J., and Gillaspy,  
777 G.E. (2009). VTC4 is a bifunctional enzyme that affects myoinositol and  
778 ascorbate biosynthesis in plants. *Plant physiology* 150:951-961.  
779 Ward, J.T., Lahner, B., Yakubova, E., Salt, D.E., and Raghothama, K.G. (2008). The  
780 effect of iron on the primary root elongation of *Arabidopsis* during phosphate  
781 deficiency. *Plant Physiology* 147:1181-1191.  
782 White, P.J., and Broadley, M.R. (2009). Biofortification of crops with seven mineral  
783 elements often lacking in human diets—iron, zinc, copper, calcium, magnesium,  
784 selenium and iodine. *New Phytologist* 182:49-84.  
785 Zhao, Q., Wu, Y., Gao, L., Ma, J., Li, C.Y., and Xiang, C.B. (2014). Sulfur nutrient  
786 availability regulates root elongation by affecting root indole-3-acetic acid  
787 levels and the stem cell niche. *Journal of integrative plant biology* 56:1151-  
788 1163.  
789 Zhu, C., Kobayashi, K., Loladze, I., Zhu, J., Jiang, Q., Xu, X., Liu, G., Seneweera, S.,  
790 Ebi, K.L., and Drewnowski, A. (2018). Carbon dioxide (CO<sub>2</sub>) levels this century  
791 will alter the protein, micronutrients, and vitamin content of rice grains with  
792 potential health consequences for the poorest rice-dependent countries.  
793 *Science advances* 4:eaaq1012.  
794  
795

## 796 Acknowledgment

797 The authors are thankful to Bonnie Wohlrab and Christian Göschl for technical  
798 assistance. This work was funded by the “Institut National de la Recherche  
799 Agronomique – Montpellier - France” INRA and by the AgreeenSkills Plus to H.R.,  
800 and supported by funds from the Austrian Academy of Science through the Gregor  
801 Mendel Institute (GMI) to W.B., an Austrian Science Fund (FWF) stand-alone project  
802 (P27163-B22) to W.B., and by the National Institute of General Medical Sciences of  
803 the National Institutes of Health (grant number R01GM127759 to W.B.), and  
804 supported by funds from the Carnegie Institution for Science and Brigitte Berthelemon  
805 to S.Y.R.

806

## 807 Author Contributions

808 H.R. coordinated the project and writing of the manuscript. H.R. and W.B. designed  
809 the GWAS. N.B. and S.B.S. carried out the experiments. A.K. performed the GWAS  
810 analysis. S.Y.R. and H.R. conceived data analysis scheme, analyzed the data, and  
811 formulated the manuscript.

812

813 **Declaration of interest**

814 The authors declare no competing financial interests.

815

816

817

818 **Supplemental Tables**

819

820 **Supplemental Table 1.** Primary root length and root growth rate (RGR) of 227  
821 natural accessions of *Arabidopsis thaliana* grown on control condition (Ct), deficiency  
822 of phosphorus (-P), iron (-Fe), zinc (-Zn), phosphorus and iron (-P-Fe), or  
823 phosphorus and zinc (-P-Zn). Measurements were done on 3, 4 and 5 days-old  
824 seedlings.

825

826

827 **Supplemental Table 2.** Normalized root growth rate (RGR) of the 227 natural  
828 *Arabidopsis thaliana* accessions. Values were obtained by diving the RGR presented  
829 in Supplemental Table 2 for each of the nutrient-deficient conditions with the RGR  
830 under control condition (Ct).

831

832 **Supplemental Table 3.** Heritability estimates for the root growth rate (RGR) and the  
833 normalized RGR using estimates from the linear mixed model.

834

835 **Supplemental Table 4.** List of 145 candidate genes that are present in a 10kb  
836 window around significant SNPs for the GWAS of normalized root growth rate (RGR)  
837 under nutrient-deficient conditions. The threshold used to declare these SNPs  
838 significant is Bonferroni.

839

840 **Supplemental Table 5.** List of 87 significant SNPs for the GWAS of normalized root  
841 growth rate (RGR) under the different nutrient-deficient conditions and the genes that  
842 are surrounding these SNPs

843

844 **Supplemental Table 6.** List of 21 candidate genes found in the analyses of root  
845 growth rate (RGR) of phosphorus and iron deficiency (-P-Fe) normalized on iron  
846 deficiency (-Fe).

847  
848 **Supplemental Table 7.** List of candidate genes found in the GWAS analyses  
849 (threshold of  $p=10^{-4}$ ) of root growth rate (RGR) of phosphorus and iron deficiency (-P-  
850 Fe) normalized on iron deficiency (-Fe) and phosphorus and zinc deficiency (-P-Zn)  
851 normalized on zinc deficiency (-Zn) .

852  
853 **Supplemental Table 8.** List of 31 SNPs that are found in the GWAS analyses  
854 (threshold of  $p=10^{-4}$ ) of RGR of phosphorus and iron deficiency (-P-Fe) normalized  
855 on iron deficiency (-Fe) and phosphorus and zinc deficiency (-P-Zn) normalized on  
856 zinc deficiency (-Zn).

857  
858 **Supplemental Table 9.** List of 10 genes that are found in both, the analyses of RGR  
859 of phosphorus and iron deficiency (-P-Fe) normalized on iron deficiency (-Fe) and  
860 phosphorus and zinc deficiency (-P-Zn) normalized on zinc deficiency (-Zn) at a less  
861 stringent threshold of  $p=10^{-4}$ .

862  
863 **Supplemental Table 10.** List of genes forming the modules identified through the  
864 analyses of GWAS candidate genes for  $\Delta\text{RGR}_{(-\text{P-Fe}, -\text{Fe})}$  and for  $\Delta\text{RGR}_{(-\text{P-Zn}, -\text{Zn})}$  traits  
865 using the publicly available resources, AraNet.

866

867 **Figure legend.**

868

869 **Figure 1. A systems framework to study root growth under mineral limitation**

870 (A) Design of the experimental set up. 227 *Arabidopsis thaliana* accessions were  
871 grown on vertical agar plates containing different media, including control (Ct),  
872 deficiency of phosphorus (-P), iron (-Fe), zinc (-Zn), phosphorus and iron (-P-Fe), or  
873 phosphorus and zinc (-P-Zn). Seedlings were daily imaged and primary root length  
874 (PRL) of 3-, 4-, 5-day-old seedlings was determined. (B) The root growth rate (RGR)  
875 was determined by conducting linear regression on PRL of twelve replicates per  
876 accession and for each treatment. Five GWAS were performed using on normalized  
877 RGRs, which were obtained for each accession by calculating the ratio between  
878 RGR on each nutrient deficiency condition divided by the value on the control  
879 condition (Ct). GWAS was also performed on the variation of normalized RGR on -P-  
880 Fe and -Fe, or -P-Zn and -Zn by the value on control condition (Ct) and expressed

881 as  $\Delta RGR_{(-P-Fe, -Fe)} = RGR_{(-P-Fe/Ct)} - RGR_{(-Fe/Ct)}$ , and for -P-Zn and -Zn  $\Delta RGR_{(-P-Zn, -Zn)} =$   
882  $RGR_{(-P-Zn/Ct)} - RGR_{(-Zn/Ct)}$ . (C) The significance of associations between phenotypes  
883 and the single nucleotide polymorphisms (SNPs) markers was evaluated using linear  
884 mixed model. The GWAS candidate genes for a given RGR trait were used to identify  
885 a gene connected with one another, which form a molecular pathway, using a  
886 machine learning algorithms to infer co-functional links from genomics data, AraNet  
887 (Lee et al., 2015).

888  
889 **Figure 2. Effect of single and double deficiencies of iron, zinc and phosphorus**  
890 **on the primary root elongation of the *Arabidopsis thaliana* reference accession**  
891 **Col-0** Seeds of the *A. thaliana* Col-0 accession were germinated on six different  
892 nutrient conditions: control (Ct), deficiency of P (-P), Fe (-Fe), Zn (-Zn), P and Fe (-P-  
893 Fe), and P and Zn (-P-Zn). The primary root length was determined on 3-, 4-, and 5-  
894 day-old seedlings.

895  
896 **Figure 3. Natural variation of 227 *Arabidopsis thaliana* accessions in their**  
897 **responses to single and double deficiencies in iron, zinc and phosphorus (A)**  
898 Relationship between root growth rate (RGR) under phosphate deficiency (-P) and  
899 RGR under control condition (Ct). (B) Relationship between RGR under iron  
900 deficiency (-Fe) and root growth in Ct. (C) Relationship between RGR under zinc  
901 deficiency (-Zn) and RGR in Ct. (D) Relationship between RGR in -P-Fe and RGR in  
902 Ct. (D) Relationship between root growth rate under in -P-Zn and RGR in Ct. Each  
903 data point represents the RGR estimated from a pool of plants (median n in each  
904 treatment > 10). The solid black dot represents the Col-0 reference accession. The  
905 solid black line represents the diagonal (i.e. the growth that would be expected  
906 without any response) and not the results of a regression analysis.

907  
908 **Figure 4. Genetic architectures of root growth rate control in response to**  
909 **single and double deficiencies of iron, zinc and phosphorus from GWAS (A-E)**  
910 Genome-wide distribution of the  $-\log_{10}$  P-values of SNP/phenotype associations  
911 using a linear mixed model method that corrects for population structure (AMM).  
912 SNPs associated with the root growth rate under the deficiency of -P (A), -Fe (B) -Zn  
913 (C), -P-Fe (D), or -P-Zn (E) compared to control condition (Ct) are presented. SNPs  
914 are plotted according to their position along the chromosomes. Plotting colors  
915 alternate between black and grey in order to facilitate the visualization of each of the  
916 five chromosomes. 5% Bonferroni threshold is indicated by black dashed line. (F)

917 Van Diagram of GWAS candidate genes underlying *Arabidopsis* RGR under the  
918 different nutrient-deficient conditions: -P, -Fe, -Zn, -P-Fe and -P-Zn conditions. The  
919 Van diagram was generated using a web-based tool for the analysis of sets through  
920 Venn diagrams (InteractiVenn) (Heberle et al., 2015).

921  
922 **Figure 5. P deficiency suppresses negative effects of Fe and Zn deficiency on**  
923 **the root growth rate of most *Arabidopsis thaliana* accessions** The root growth  
924 rate (RGR) of 227 accessions of *Arabidopsis thaliana* grown under each of the  
925 nutrient-deficient conditions was normalized to the corresponding values under  
926 control conditions (Ct). (A) Relationship between RGR under combined phosphorus  
927 and iron deficiency (-P-Fe/Ct) and RGR under phosphorus deficiency (-P/Ct). The  
928 red dots represent the ecotypes that showed limited RGR by -P considering one  
929 standard deviation away from the mean with 15.8% confidence limit to the RGR data,  
930 and which are promoted in -P-Fe. (B) Relationship between RGR under phosphorus  
931 and iron deficiency (-P-Fe/Ct) and RGR under iron deficiency (-Fe/Ct). (C)  
932 Relationship between root RGR under phosphorus and zinc deficiency (-P-Zn/Ct)  
933 and RGR under zinc deficiency (-Zn/Ct). Each data point was obtained from the  
934 analysis of RGR from a pool of plants ( $n \geq 9$ ). The solid black dot represents the Col-  
935 0 ecotype. The solid black lines represent the diagonal.

936  
937 **Figure 6. Combined phosphorus and zinc deficiency promotes root growth rate**  
938 **of most *Arabidopsis thaliana* accessions** Representative images of contrasting  
939 primary root growth phenotype (5 days) of four *Arabidopsis thaliana* accessions  
940 (Shadara, Sq-1, Sapporo-0, Si-0) grown on vertical agar plates in the presence of  
941 zinc (+Zn), in the absence of zinc (-Zn), or the absence of both phosphorus and zinc  
942 (-P-Zn).

943  
944 **Figure 7. Compensation of root growth rate by nutrient limitation interactions**  
945 **and Manhattan plots of GWAS results** (A-B) Variation in the root growth rate  
946 (RGR) between -P-Fe and -Fe compared to control condition (Ct) presented as  
947  $\Delta RGR_{(-P-Fe, -Fe)} = ((-P-Fe/Ct) - RGR(-Fe/Ct))$ , and (B) between -P-Zn and -Zn  
948 compared to control condition (Ct)-P-Zn and -Zn presented as  $\Delta RGR_{(-P-Zn, -Zn)} = ((-P-$   
949  $Zn/Ct) - RGR(-Zn/Ct))$ . (C) SNPs associated with the  $\Delta RGR_{(-P-Fe, -Fe)}$  or (D)  $\Delta RGR_{(-P-$   
950  $Zn, -Zn)}$ . SNPs are plotted according to their position along the appropriate  
951 chromosome. Plotting colors alternate between black and grey in order to facilitate  
952 the visualization of each of the five chromosomes. Bonferroni threshold is indicated

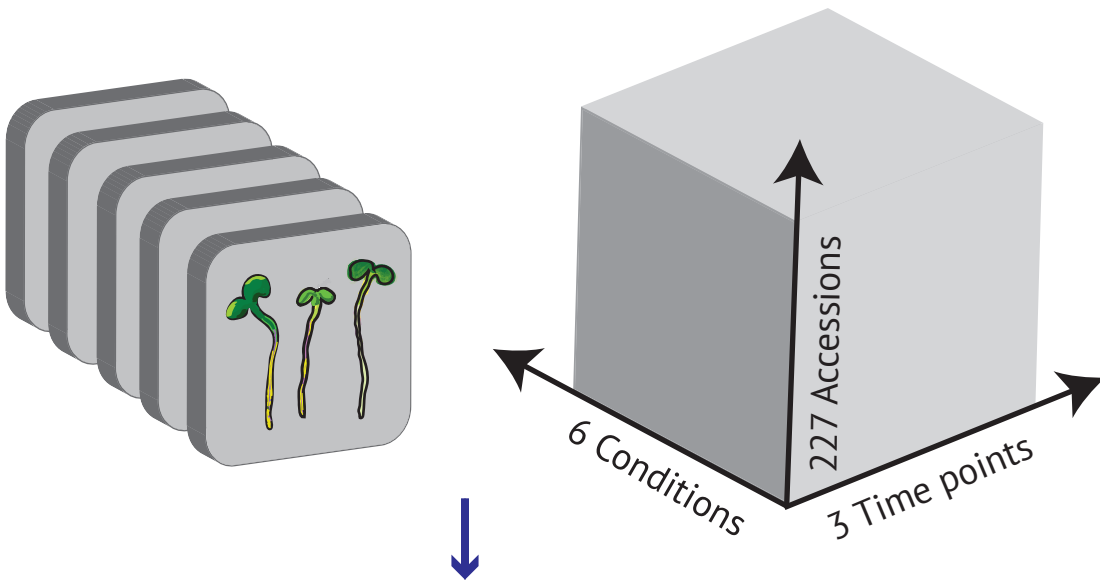
953 by black dashed line. (C-D) Genome-wide distribution of the  $-\log_{10}$  P-values of  
954 SNP/phenotype associations using the MMA method.

955

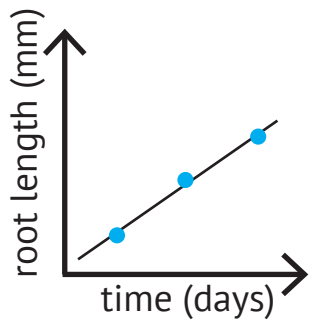
956 **Figure 8. Predicted molecular pathway for the compensation of root growth**  
957 **rate by phosphate and iron combined stresses** A network between the subset of  
958 the GWAS candidate genes identified using the publicly available resource AraNet  
959 (Lee et al., 2015). The network visualization is generated using Cytoscape software  
960 (Shannon et al., 2003). The Gene Ontology (GO)-biological process enrichment of a  
961 subset list of GWAS genes for  $\Delta RGR_{(-P-Fe, -Fe)}$  were conducted using AraNet. Genes  
962 enriched in GO terms are marked with stars: “chromatin modification” (blue), “DNA  
963 replication” (red), and “regulation of cell cycle” (green).

## Figure 1

### A High-throughput, multi-dimensional phenotyping

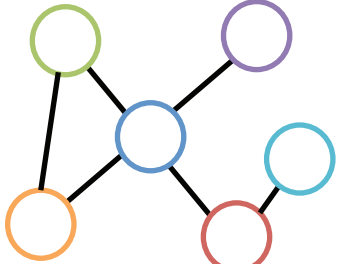


### B Automated root image analysis



root growth rate (RGR)  $R = \text{root length}/\text{time}$   
normalized RGR  $NR = R(\text{treatment})/R(\text{control})$   
compensated RGR  $= NR(\text{dual treatments}) - NR(\text{single treatment})$

### C Network analysis



### GWAS

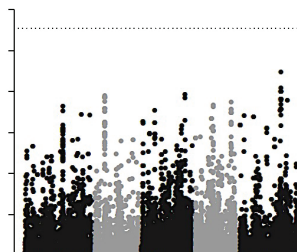
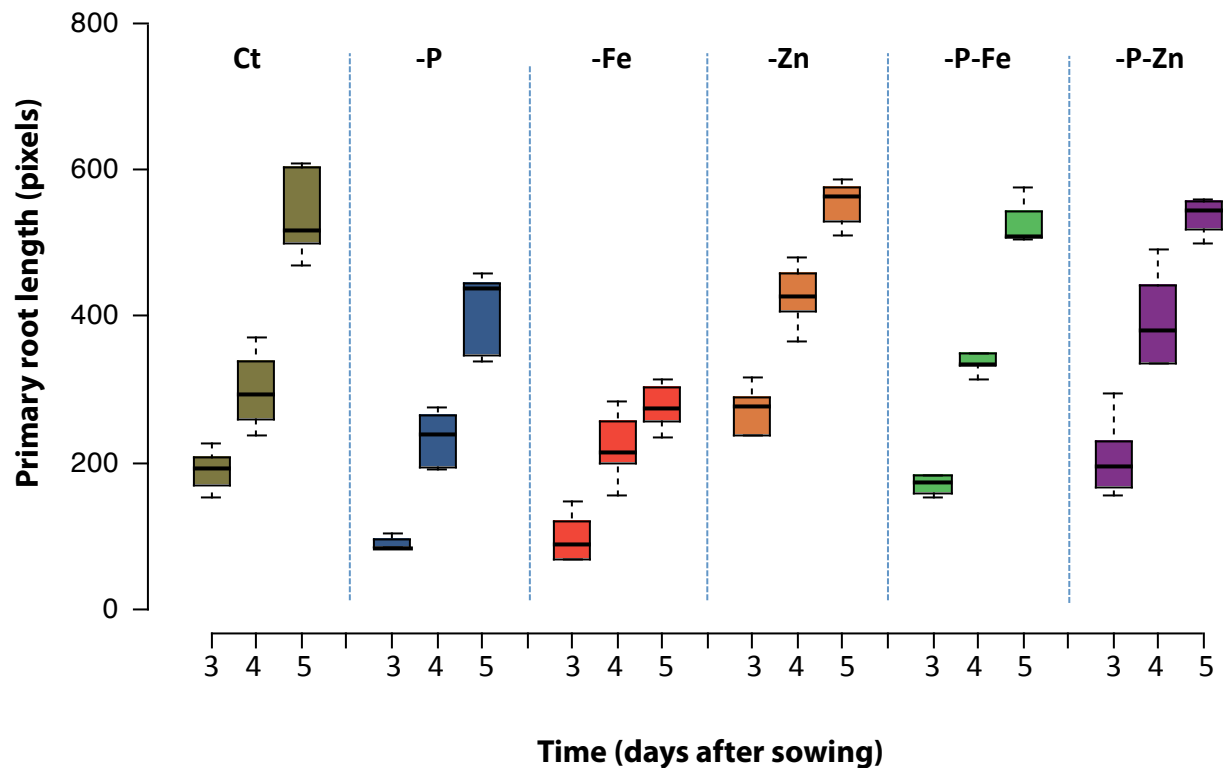
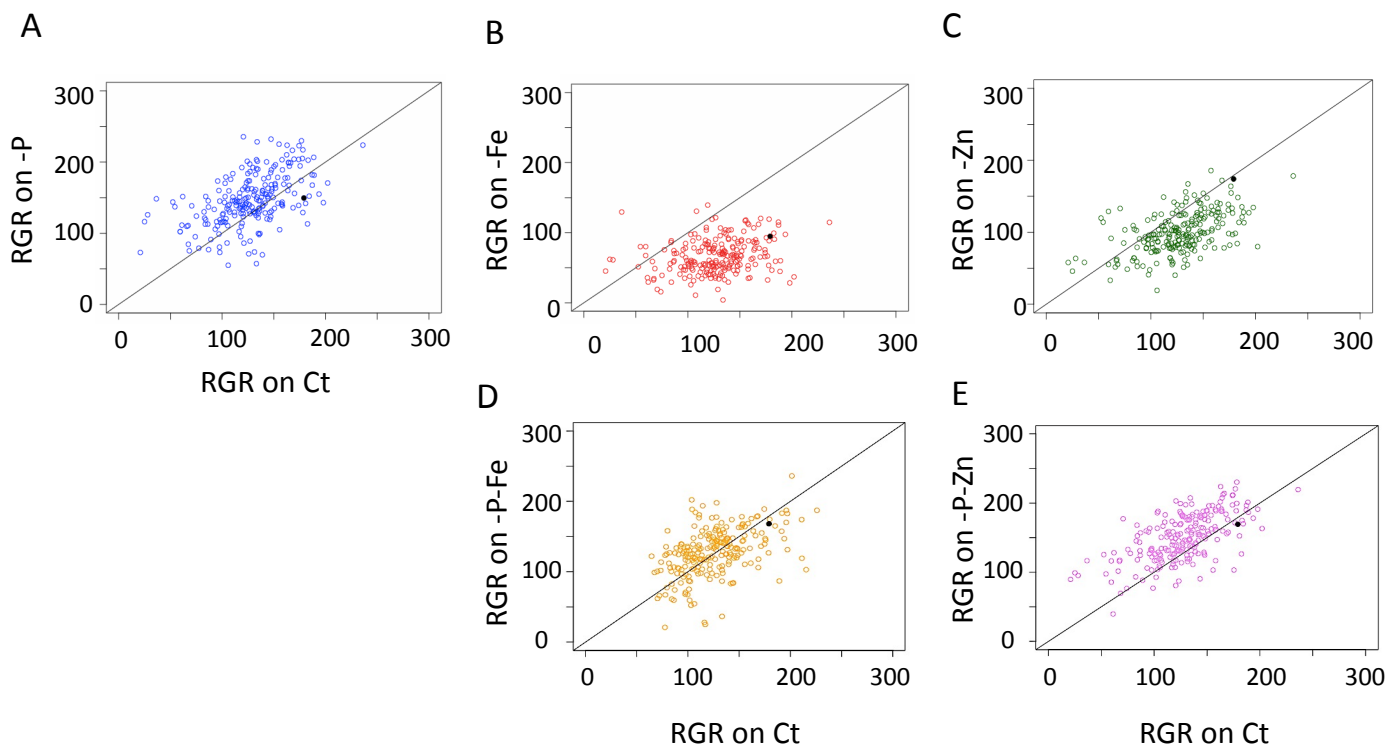


Figure 2



**Figure 3**



**Figure 4**

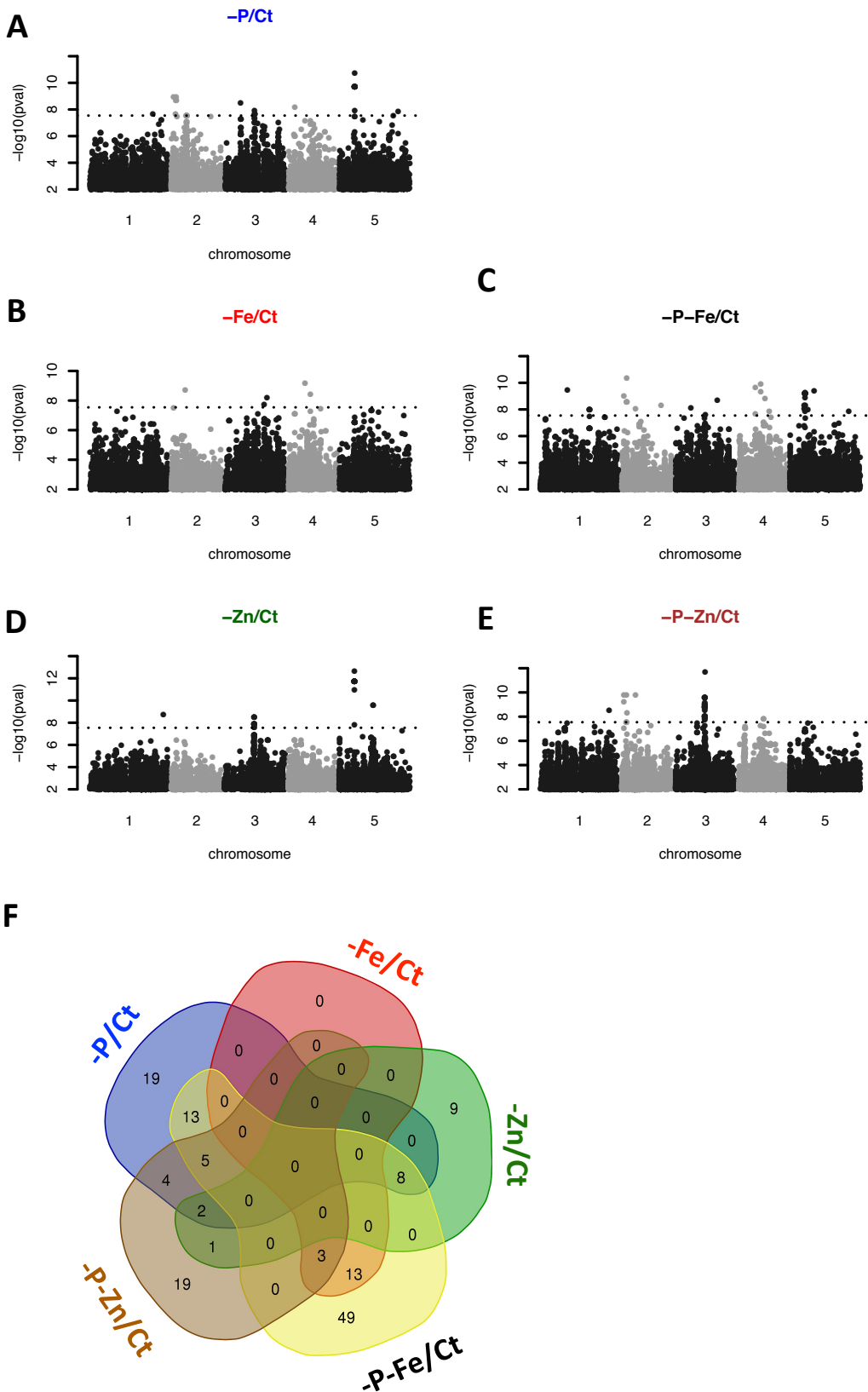
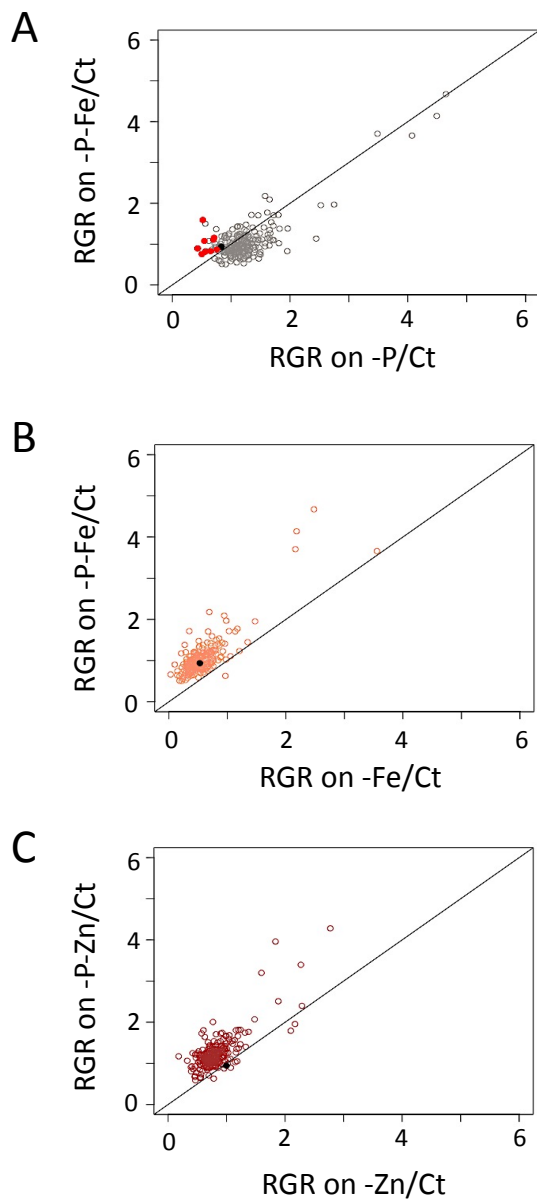
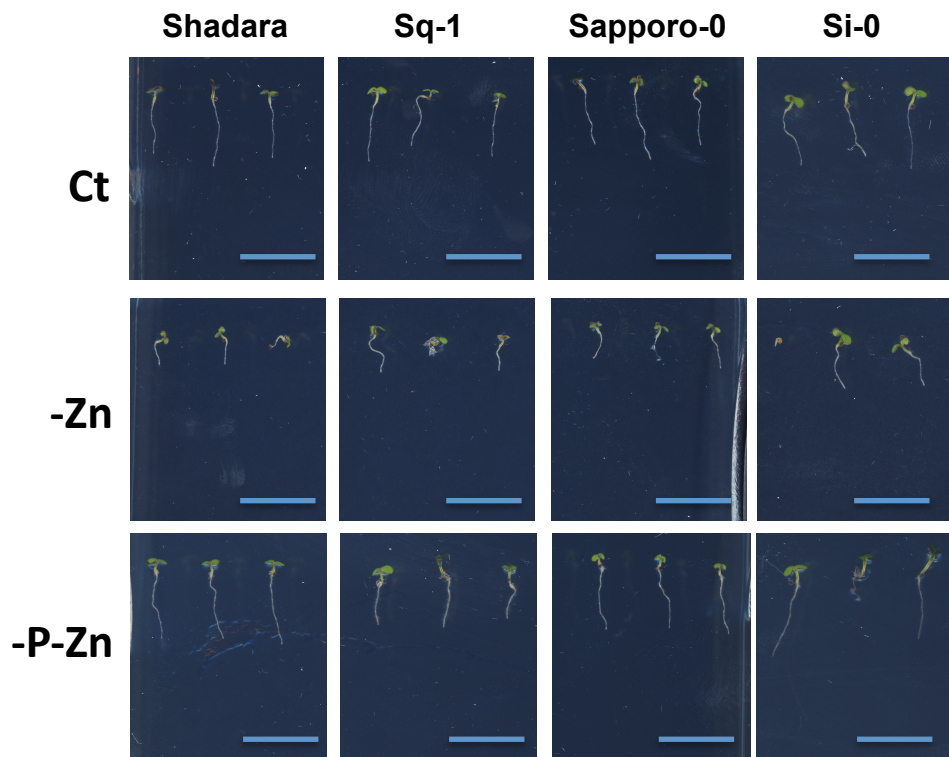


Figure 5

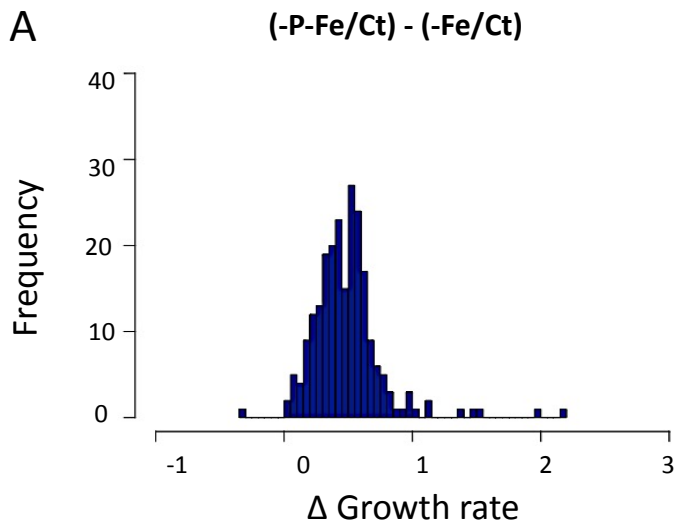


**Figure 6**

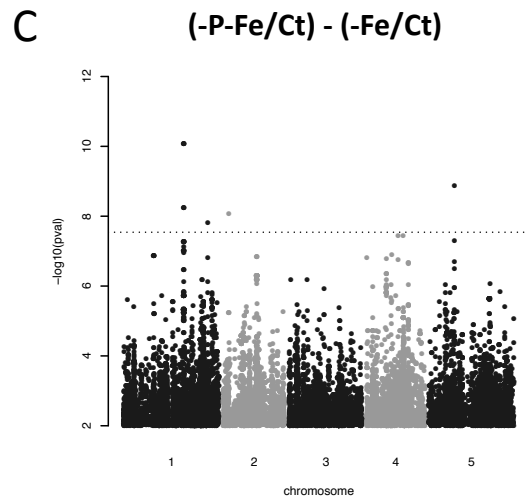


**Figure 7**

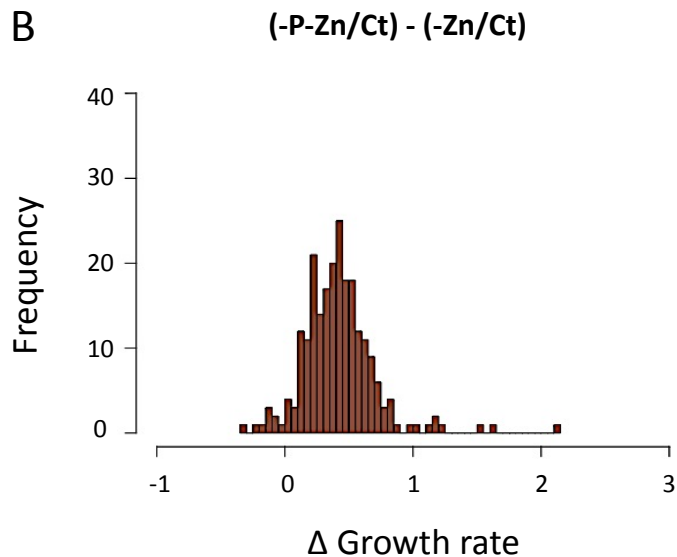
**A**



**C**



**B**



**D**

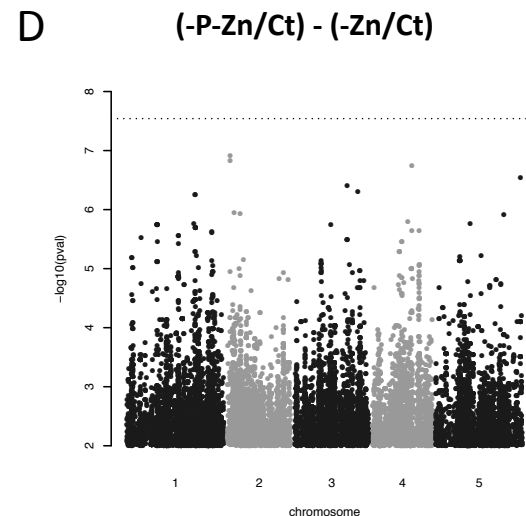


Figure 8

bioRxiv preprint doi: <https://doi.org/10.1101/460360>; this version posted November 4, 2018. The copyright holder for this preprint (which was not certified by peer review) is the author/funder. All rights reserved. No reuse allowed without permission.

